Acetaminophen metabolism revisited using non-targeted analyses: implications for human biomonitoring

Arthur David[1]*, Jade Chaker[1], Thibaut Léger[1], Raghad Al-Salhi[1], Marlen D. Dalgaard[2], Bjarne Styrishave[3], Daniel Bury[4], Holger M. Koch[4], Bernard Jégou[1,¤], David M. Kristensen[1,5,¤]

Affiliations:
[1]Univ Rennes, Inserm, EHESP, Irset (Institut de recherche en santé, environnement et travail) - UMR_S 1085, F-35000 Rennes, France.
[2]Department of Health Technology, Technical University of Denmark, Denmark.
[3]Department of Pharmacy, Faculty of Health and Medical Sciences, University of Copenhagen, Denmark.
[4]Institute for Prevention and Occupational Medicine of the German Social Accident Insurance – Institute of the Ruhr-University Bochum (IPA), Bürkle-de-la-Camp-Platz 1, 44789 Bochum, Germany.
[5]Danish Headache Center, Department of Neurology, Rigshospitalet-Glostrup, Denmark.

*Corresponding author: Arthur David (arthur.david@ehesp.fr)
[¤]Joint last authors

Abstract: The analgesic paracetamol (N-acetyl-4-aminophenol, APAP) is commonly used to relieve pain, fever and malaise. While sales have increased worldwide, a growing body of experimental and epidemiological evidence has suggested APAP as a possible risk factor for various health disorders in humans. To perform internal exposure-based risk assessment, the use of accurate and optimized biomonitoring methods is critical. However, retrospectively assessing pharmaceutical use of APAP in humans is challenging because of its short half-life. The objective of this study was to address the key biomonitoring issues with APAP using current standard analytical methods based on urinary analyses of free APAP and its phase II conjugates. Using non-targeted analyses based on high-resolution mass spectrometry, we identified, in a controlled longitudinal exposure study with male volunteers, unrecognized APAP metabolites with delayed formation and excretion rates. We postulate that these metabolites are formed via the thiomethyl shunt after the enterohepatic circulation as already observed in rodents. Importantly, the conjugated thiomethyl metabolites were (i) of comparable diagnostic sensitivity as the free APAP and its phase II conjugates detected by current methods; (ii) had delayed peak levels in blood and urine compared to other APAP metabolites and therefore potentially extend the window of exposure assessment; and (iii) provide relevant information regarding metabolic pathways of interest from a toxicological point of view. Including these metabolites in future APAP biomonitoring methods therefore provides an option to decrease potential underestimation of APAP use and challenges the notion that the standard methods in biomonitoring based exclusively on the parent compound and its phase II metabolites are adequate for human biomonitoring of a non-persistent chemical such as APAP.

Key words

Paracetamol/acetaminophen; human biomonitoring, non-targeted analyses, high-resolution mass spectrometry (HRMS).

Chemical abbreviations

APAP=acetaminophen; APAP-S=APAP sulfate; APAP-Glu=APAP glucuronide; NAPQI=N-acetyl-*p*-benzoquinone imine; 3-OH-APAP=3-hydroxyacetaminophen; 3-OH-APAP-S=3-hydroxyacetaminophen sulfate; 3-OCH_3-APAP=3-methoxyacetaminophen; 3-OCH_3-APAP-Glu=3-methoxyacetaminophen glucuronide; APAP-SG=acetaminophen glutathione; APAP-Cys= 3-(Cystein-S-yl)acetaminophen ; NAC-APAP= Acetaminophen mercapturate; NAC-O-APAP= Acetaminophen mercapturate sulfoxide; SH-APAP= 3-mercaptoacetaminophen; SH-APAP-Glu= 3-mercaptoacetaminophen glucuronide; SH-APAP-S= 3-mercaptoacetaminophen sulfate; S-CH_3-APAP= S-methyl-3-thioacetaminophen; S-CH_3-APAP-S= S-methyl-3-thioacetaminophen sulfate; S-CH_3-APAP-Glu= S-methyl-3-thioacetaminophen glucuronide; SO-CH_3-APAP= S-methyl-3-thioacetaminophen sulphoxide ; SO-CH_3-APAP-S= S-methyl-3-thioacetaminophen sulphoxide sulfate; SO-CH_3-APAP-Glu= S-methyl-3-thioacetaminophen glucuronide.

INTRODUCTION

The mild analgesic paracetamol/acetaminophen (N-acetyl-4-aminophenol, APAP) is an active ingredient in more than 600 prescription and non-prescription pharmaceuticals (Hurwitz et al., 2014). This analgesic is one of the most commonly used pharmaceuticals worldwide, with sales that have steadily increased over the past 20 years in several countries (Kristensen et al., 2016). The medical benefits of APAP are widely recognized; APAP can be used on its own, in mixed formulations or even as an alternative to non-steroidal anti-inflammatory drugs whose suspected negative side effects have raised concerns (Kristensen et al., 2018). However, recent experimental as well as epidemiological studies suggest APAP as a possible risk factor for male developmental disorders in humans, on its own, or in combination with other reproductive and developmental toxicants (Albert et al., 2013; Konkel, 2018; Kortenkamp, 2020; Kortenkamp and Koch, 2020; Kristensen et al., 2012; Kristensen et al., 2016). Furthermore, incorrect use of APAP is strongly associated with a broad spectrum of side effects and is the most common cause of acute liver failure (fulminant liver failure) with over 100,000 cases alone in the US (Ferri, 2016).

Besides APAP exposure through intentional pharmaceutical use, it has been shown that APAP is ubiquitously excreted in the urine of non-users in the general population (medians of 61.7 µg/L and 100 µg/L from the German (men and women) (Modick et al., 2014) and Danish (women and children) (Nielsen et al., 2015) populations, respectively), indicating that an unintentional environmental exposure exists. The environmental exposure has been linked to APAP precursors such as aniline and 4-aminophenol (two large-volume intermediates in industrial processes) and/or indirect APAP exposure (Kristensen et al., 2016; Modick et al., 2014; Modick et al., 2016). The APAP urinary background concentrations measured in non-users are about 4000 fold lower than the maximum urinary concentrations measured after oral intake of 500 mg APAP, but in the range of concentrations measured 24-48h after such an intentional oral intake (Modick et al., 2014). Hence, these environmental APAP urinary concentrations can interfere when assessing APAP use in epidemiological studies especially if intentional APAP intake occurred >24h before sampling.

Understanding the amount of a chemical that enters the human body, whether from intentional use or unintentional exposure, is essential for both exposure and risk assessment. APAP metabolism is rapid (half-life <3h in blood (Mazaleuskaya et al., 2015)) and the large majority of the APAP therapeutic dose is classically believed to be excreted in urine as direct phase II glucuronide and sulfate conjugates. Mercapturic acid and cysteine conjugates derived from glutathione conjugation of the reactive metabolite N-acetyl-p-benzoquinone imine (NAPQI) are also produced in APAP metabolism. However, these metabolites are generally considered as minor metabolites together with catechol metabolites produced by CYP450 enzymes (Bessems and Vermeulen, 2001; Mazaleuskaya et al., 2015). Thus, present standard targeted methods analyzing free APAP and the phase II conjugates as "total APAP" after enzymatic deconjugation have been considered as the valid standard methods for estimating internal exposure for risk assessment purposes (Bornehag et al., 2018; Modick et al., 2014; Nielsen et al., 2015). However, these methods capture only part of the metabolic pathway and a relatively short time window to assess APAP origin (i.e. pharmaceutical use versus environmental), leading to potential underestimations of actual exposures. Exposure underestimations may have large implications as they could fundamentally compromise outcomes of risk assessment decisions.

In this study, we address the key issue of potential underestimation of APAP use using current human-biomonitoring methods focused on free APAP and phase II conjugates, only. We monitored APAP exposure over four days in blood and urine of four male volunteers with an administration of 1 gram of APAP on the third day. Using recent untargeted technological advancements of high-resolution mass spectrometry (HRMS) combined with omics-based data treatment, we investigated the presence of up to now largely neglected APAP metabolites from enterohepatic circulation with formation and excretion times potentially longer than APAP. Such additional knowledge can improve the human

biomonitoring approach for the non-persistent chemical APAP in future exposure and risk assessment studies.

MATERIALS AND METHODS

Longitudinal clinical trial

Design and participants

The human in vivo study (n=4) was designed as a longitudinal exposure to APAP over four days with an administration of 1 gram of APAP on the third day (Fig S1.). The study protocol was in compliance with the Helsinki Declaration and was approved by the Regional Scientific Ethical Committees of Copenhagen in Denmark (Protocol nr.: 17003845; and as part of trial H-17002476). The study recruited 4 healthy men aged 30-60 years at the Department of Pharmacy and Department of Biology, University of Copenhagen. Exclusion criteria include other use of medicine and body mass index above 30, peptic ulcers, signs of liver or kidney dysfunction. All individuals provided oral informed consent to participate in the study.

Collection of blood plasma and urine samples before and after APAP intake

The subjects received APAP 2 × 500 mg (Panodil®, GlaxoSmithKline Aps). No subjects reported any adverse signs of taking the medication. Three baseline samples of urine (spot urine) and plasma were sampled in the morning two days and just prior to intake of APAP. Subsequently, samples were taken +1h, +2h (urine only), +4h, +6h hours after intake and in the morning of the subsequent two days (+24 and 48h). For each time point, 10-mL heparinized blood samples were collected from the antecubital vein of the non-dominant arm together with urine samples. Blood samples were centrifuged (5 min, 10,000 g) and plasma collected. Plasma and urine samples were stored at −80 °C immediately after collection.

Targeted analyses of APAP in blood plasma and urine

APAP was analyzed using an adapted version of a method previously described (Modick et al., 2013; Modick et al., 2016). Unlabeled APAP (NA4AP) was used for calibration (the mass transition *m/z* 152 → 110 was used for quantification and *m/z* 152 → 93 was used as qualifier) and APAP-d_4 (NA4AP-d_4) was used as internal standard (same mass transitions as reported in Modick et al. (Modick et al., 2016)). The gradient for the analytical separation was modified, starting at 15% solvent B (acetonitrile containing 0.05% formic acid). After 0.5 min, B was increased to 35% within 0.5 min and then increased to 45% within 3.5 min. Afterwards, B was increased to 50% within 1.5 min and then to 95% within 2 min and kept for 2.5 min. B was then returned to initial 15% within 2.5 min and kept for 3 min. Furthermore, the curtain gas pressure was increased from 25 to 35 psi to reduce contaminations of the ion path. The limit of quantification (based on a signal-to-noise ratio of 10) was 1 µg/L APAP. Plasma samples were analyzed at least in 2-fold dilution (diluted with water). Urine concentrations were normalized to specific gravity measured using a refractometer (Atago Urine S.G. scale : 1.000 to 1.060).

Non-targeted analyses of APAP in blood plasma and urine

- *Chemicals*

The list of standards used for the identification of APAP metabolites and the 15 labelled internal standards (IS) spiked in samples for the untargeted analyses and their respective suppliers are provided in Table S1. All solvents were high-performance liquid chromatography grade, purchased from Biosolve Chime (Dieuze, France). Phree Phospholipid Removal 96-well plates and Strata-X Polymeric Reversed Phase cartridges (200 mg, 3 mL) were supplied by Phenomenex (Le Pecq, France).

- *Preparation of blood plasma and urine samples*

Plasma samples were prepared based on the method published in David et al. (David et al., 2014) Previous studies have demonstrated that this sample preparation method developed for untargeted analysis purposes using phospholipid removal followed by polymeric reversed phase solid phase extraction extracts xenobiotics such as pharmaceuticals (including APAP), conjugated xenobiotics as well as non-polar, cationic and anionic metabolites (e.g., steroids, eicosanoids, amino acids, neurotransmitters, bile acids and lipids) from plasma samples (David et al., 2014; David et al., 2017). Urine samples were prepared using a similar SPE protocol as the one used for the plasma. The step before SPE, i.e. removal of phospholipid and protein using the Phree plates, was omitted as urine contains lower levels of these molecules (as opposed to plasma). Previous studies have shown that methods using polymeric SPE are efficient to concentrate urine samples for untargeted analyses and extract the urinary metabolome and (xeno)metabolome (Chetwynd et al., 2015)

- *UHPLC-ESI-QTOFMS analyses*

Plasma and urine extracts were profiled using an Exon UHPLC system (AB Sciex, USA) coupled to an AB Sciex X500R Q-TOF-MS system (Sciex technologies, Canada), equipped with a DuoSpray ion source. 2 µL of extracts were loaded and separated on an Acquity UHPLC HSS-T3 column, 1.0 mm x 150 mm x 1.8 µm, maintained at 40°C (Waters Technologies, Saint Quentin, France). HPLC grade water was used as solvent A and acetonitrile as solvent B, both modified with 0.01% formic acid. The flow rate was 100 uL/min with a gradient of 0-2.5 min from 10% to 20% B, 2.5-20 min from 20 to 30% B, 20-38 min from 30% to 45% B, 38-45 min from 45 to 100% B, 45-55 min 100% B, and equilibration to initial conditions in 5 min.

The Q-TOF was recalibrated automatically after each measurement using an ESI positive/negative calibration solution via a calibration delivery system (CDS). Samples were analysed in full scan experiment (50-1100 Da) in both – and + ESI modes. The common parameters in both positive/negative ion modes were: collision energy, 10 eV; curtain gas, 35; ion source gas 1, 50; ion source gas 2, 70; temperature, 550°C; declustering potential, 80 V; mass resolution of 50,000.

MS/MS mass fragmentation information for chemical elucidation was obtained by further analysis of selected samples in sequential window acquisition of theoretical mass spectrum (SWATH). Swath data-independent acquisitions were performed in order to achieve comprehensive MS/MS sampling. The Q1 isolation window strategy was generated using the Sciex Variable Window Table from previously acquired MS data on the specific sample of interest in order to optimize window widths across the entire *m/z* range. SWATH experiments were performed in both – and + mode with parameters: MS1 accumulation time, 80 ms; MS2 accumulation time, 30 ms; collision energy, 35 eV; collision energy spread, 15 eV; cycle time, 469 ms; mass range, m/z 50–900.

- *Quality Control.*

For the untargeted analysis, one workup blank sample (i.e., extraction with HPLC grade water instead of sample) per analytical batch was prepared to monitor for background contaminants. Quality control (QC) samples comprising a composite sample were prepared in order to monitor for UHPLC-ESI-TOF-MS repeatability and sensitivity during analysis of a sample run. Solvent blank samples (acetonitrile/H_2O (20:80)) were also injected to ensure that there was no carryover in the UHPLC system that might affect adjacent results in analytical runs. Each run commenced with the injection of the blank samples (workup and solvent) followed by injection of a QC sample. The samples were injected randomly with QC samples analyzed after every 7 samples for plasma and 5 samples for urine. To assess the UHPLC-ESI-Q-TOF-MS analytical variability during analytical runs, coefficients of variation (CV) for the peak areas were calculated for each IS in QC samples. Furthermore, the analytical

variability of the plasma and urine runs was also assessed based upon the method proposed by Want et al. (Want et al., 2010) The response of each marker (i.e., the area) from all QC samples was normalized to the total ion signal (area) to monitor the analytical variability at the whole metabolome scale. Using this method, mean area of more than 80% of all markers present in QCs had CVs of less than 30% as recommended by Want et al.(Want et al., 2010) for metabolomics experiments (Table S5). Coefficients of variation (CVs) of the peak areas of each labelled internal standard (n=15) measured in quality controls (QCs) in plasma (n=6 QCs) and urine (n=9 QCs) were all below 20% (Table S5). To correct for extraction issues and matrix interferences, the peak area of each metabolite was adjusted to that of APAP-d4 in case of blood and to the total peak area (or sum of peak areas) in urine (to correct mainly for urinary dilution issues).

- *HRMS dataset*

Mass spectra collected in full scan mode (*m/z* 50−1100) and spectral peaks were preprocessed (i.e., deconvolution, alignment, peak picking) using both the open source R package XCMS (Smith et al., 2006) and vendor software MarkerView 1.3.1 (AB, Sciex) to create separate aggregate datasets from all sample files in which the MS features were binned into retention time (Rt) × *m/z* values. For XCMS, the raw data files were first converted to 64 bit .mzML (full scan) using MSConvert from ProteoWizard (Adusumilli and Mallick, 2017).

The peak tables obtained with XCMS were used for multivariate and univariate analyses in an R environment (R version 3.6.0) in order to identify APAP metabolites after APAP exposure (see Table S2 for parameters used). Principal component analyses (PCA) were performed as a first step to examine QC clustering, sample separation and identify any analytical or biological outliers (See Fig. S2 and S3). Sample groups were then defined as follows in order to perform Sparse Partial Least Squares Discriminant Analyses (sPLS-DA) models: *baseline group* = samples collected two days and just prior to intake of APAP, *1-6h group* = samples collected +1, +2, +4, +6 hours after intake and *+1-2 days group* = samples collected in the morning the subsequent two days. sPLS-DA was performed with mixOmics R package (version 6.8.5) in the mode regression (Rohart et al., 2017) (See Fig. S4 and S5). Besides multivariate analyses, univariate analyses were performed to compare fold changes of markers between the three different groups with the mixOmics R package. A corresponding p-value was calculated with the multtest R package using Unpaired Student's t-tests, with an Adaptive Benjamini and Hochberg (ABH) correction for multiple comparisons to identify markers discriminations between groups. All markers having p-value < 0.01 were selected for further tentative annotation process.

Discriminating markers between the three groups identified through multi- and univariate analyses were first screened using a list of known APAP metabolites. Identities of these expected APAP metabolites were determined from accurate mass, isotopic fit, fragmentation data obtained from SWATH acquisition and from comparison with standard compounds when available or spectra available in online libraries or the literature. In order to provide confidence in metabolite identification, we supply confidence levels based on recommendations made by Schimansky et al. (Schymanski et al., 2014) (see Supp. Table S6). The structural identities of unknown discriminating markers were determined from their accurate mass, isotopic fit, fragmentation data obtained from SWATH acquisition. These parameters were compared with those from online libraries such as PubChem (Kim et al., 2019), ChemSpider (Pence and Williams, 2010), KEGG (Kanehisa, 2002), HMDB (Wishart et al., 2018b), Metlin (Guijas et al., 2018), T3DB (Wishart et al., 2015), MassBank (Horai et al., 2010) or DrugBank (Wishart et al., 2018a). When no experimental spectra were available, MS/MS fragmentation patterns of individual markers were collected and annotation was based on online software such as MetFrag (Ruttkies et al., 2016) and CFM-ID (Djoumbou-Feunang et al., 2019)) which allow to perform *in silico* fragmentation of candidate molecules from different databases (e.g., PubChem) and search for matched against mass to charge values. When possible, chemical identity

was confirmed from accurate mass, isotopic fit and fragmentation data obtained from standard compounds (highest level of confidence).

- *Accurate integration of identified and annotated markers*

Independent peak integration and normalization were carried out to validate the significance of the discriminated metabolites between groups. All the markers identified were manually re-integrated using the Sciex OS Analytics tool. The integrated peak area of individual markers was normalized to APAP-d4 for plasma or to the total area sums for urine. Prism 8 software (GraphPad Software) was used to generate plots.

RESULTS AND DISCUSSION

Targeted analyses of APAP in blood plasma and urine

Results with targeted analyses confirmed the presence of APAP in urine (0.107 ± 0.025 mg/L, mean ± SEM, min=0.002 mg/L, max=0.200 mg/L; n =12) before the intentional APAP dose, similar to concentrations previously observed in the German (Modick et al., 2014) and the Danish populations (Nielsen et al., 2015). As illustrated in Fig 1, the peak APAP concentration in blood plasma was observed already one hour after APAP intake (mean concentration of 19.2 mg/L) in the range of plasma therapeutic concentrations previously measured (5-25 mg/L) (Schulz et al., 2012). In urine, the peak APAP concentration was observed after 4 h (mean concentration of 1.83 g/L). After 24 h and 48 h, median urinary APAP concentrations were 2.7% (mean concentration of 49.6 mg/L) and 0.3% (median concentration of 5.6 mg/L) of the maximum mean urinary concentrations, respectively.

The mean APAP urinary concentrations observed 24-48 h after APAP intake were about 50-450 fold higher than the one observed before APAP intake, but overlap with the environmental APAP concentrations previously observed in urine from the general population among non-users and non-smokers from 0.95 to 580.4 mg/L, mean=4.1 mg/L (Modick et al., 2014), confirming that, in some cases, pharmaceutical APAP use cannot be distinguished from the environmental exposure after 24 h using present standard targeted methods.

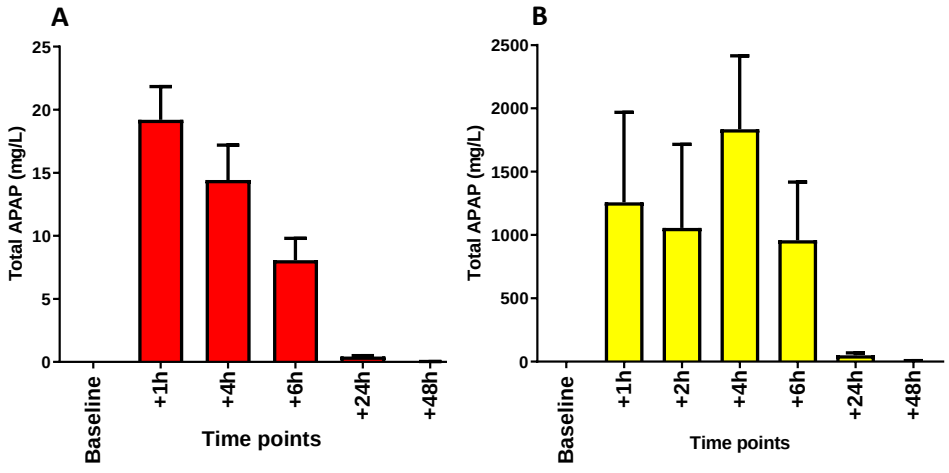

Fig. 1. "Total" APAP concentrations (free APAP, APAP glucuronide and APAP sulfate) after enzymatic deconjugation using LC-MS/MS in (A) blood plasma (mg/L, mean ± SEM) and (B) urine (mg/L, mean ± SEM) before APAP intake (baseline, n=12) and at different time points after intake. Urine concentrations are normalized to specific gravity.

Detection of new APAP metabolites in humans using HRMS-based non-targeted analyses

To gain a deeper insight into APAP metabolism, we next analyzed samples from the longitudinal exposure with a non-targeted HRMS-based method. Discriminating markers between the *baseline* group (samples collected two days and just prior APAP intake), the *+1-6h* group (samples collected from 1h up to 6h after APAP intake), and the *+1-2 days* group (samples collected in the morning of the subsequent two days after APAP intake) were identified through multi- and univariate analyses. In total, APAP and 15 of its (proposed or confirmed – see below) metabolites could be annotated and identified in blood and urine after APAP intake with confidence levels ranging from 2a-2b (annotation based on MS/MS match with experimental or *in silico* MS/MS spectrum) to 1 (confirmation of identification with a standard) according to Schymanski et al. (Schymanski et al., 2014). The list of all APAP metabolites detected in human blood and urine, their respective confidence levels, as well as the metabolic pathway involved are reported in Table 1 (see Table S6 for more information on criteria used for the annotation/identification).

Table 1. List of APAP and its metabolites detected in human blood and urine at different time points after APAP intake using high-resolution mass spectrometry. The highest level of evidence used for the annotation and identification of APAP metabolites, their respective pathway and the enzymes involved as well as previous detections in human or mammalians are reported.

List of APAP/metabolites and associated pathways	Formula	Confid. Level [1]	Higest level of evidence for identification/annotation	Main enzymes involved	Reported in humans	Reported in rodents/dogs
Parent						
APAP	C8H9NO2	**1**	Rt and MSMS match with std		yes	yes
Direct phase II reactions						
APAP-S	C8H9NO5S	**2a**	MSMS match with experimental MSMS spectra from a library [2]	STs	yes	yes
APAP-Glu	C14H17NO8	**1**	Rt and MSMS match with std	UDPGTs	yes	yes
Catechol pathway						
3-OH-APAP	C8H9NO3	**1**	Rt and MSMS match with std	CYP450	yes	yes
3-OH-APAP-S	C8H9NO6S	**2a**	MSMS match with experimental MSMS spectra from a library [2]	+STs +UDPGTs	yes	yes
3-OCH3-APAP-Glu	C15H19NO9	**2a**	MSMS match with experimental MSMS spectra from a library [2]		yes	yes
Mercapturic acid pathway						
APAP-Cys	C11H14N2O4S	**1**	Rt and MSMS match with std	CYP450 (for NAPQI)	yes	yes
NAC-APAP	C13H16N2O5S	**1**	Rt and MSMS match with std	+GSTs	yes	yes
NAC-O-APAP	C13H16N2O6S	**2b**	MSMS match with *in silico* MSMS spectra [3]	+GGTs, CGDs +NATs	no	no
Thiomethyl shunt pathway						
SH-APAP-Glu	C14H17NO8S	**2b**	MSMS match with *in silico* MSMS spectra [3]	After mercapturate pathway:	no	no
S-CH3-APAP	C9H11NO2S	**1**	Rt and MSMS match with std		yes	yes
S-CH3-APAP-S	C9H11NO5S2	**2b**	MSMS match with experimental MSMS spectra (literature) [4]	+ CS lyases + SMTs	no	yes
S-CH3-APAP-Glu	C15H19NO8S	**2b**	MSMS match with *in silico* MSMS spectra [3]	+ STs + UDPGTs	no	yes
SO-CH3-APAP-S	C9H11NO6S2	**2b**	MSMS match with *in silico* MSMS spectra [3]		no	only as unconjugated
SO-CH3-APAP-Glu	C15H19NO9S	**2b**	MSMS match with *in silico* MSMS spectra [3]		no	only as unconjugated

[1] Schimansky et al., 2014; [2] Metlin, HMDB; [3] MetFrag and CFM-ID; [4] Patterson et al., 2013. STs= sulfotransferases; UDPGTs= uridine diphosphoglucuronyltransferases; GSTs= glutathione *S*-transferases; GGTs= gamma glutamyltransferases, CGDs= cysteinylglycine dipeptidases; NATs= N-acetyltransferases; CS lyases = Cysteine S-conjugate β-lyases; SMTs= S-methyl-transferases

Based on relative peak areas, the main APAP metabolites detected in blood and urine samples collected *+1-6h* after APAP intake include direct phase II glucuronide (APAP-Glu) and sulfate (APAP-S) conjugates. APAP-Glu and APAP-S are formed by direct glucuronidation and sulfation of APAP in the liver through the action of sulfotransferases (ST) and uridine diphosphoglucuronyltransferase (UDPGTs) (Mazaleuskaya et al., 2015). We also detected in this group glutathione-derived APAP metabolites originating from the phase I reactive NAPQI, i.e., APAP-Cys and NAC-APAP. APAP is activated in the liver to form the toxic NAPQI under the mediation of CYP450 enzymes which is then almost immediately detoxified in the liver through the action of the glutathione transferases (Bessems and Vermeulen, 2001). Glutathione conjugates are then biotransformed in the liver as APAP-Cys and then NAC-APAP through the mercapturic acid pathway by the sequential action of the γ-glutamyltransferases, dipeptidases, and cysteine *S*-conjugate *N*-acetyltransferase (Hanna and Anders, 2019). Finally, we also detected in this *+1-6h* group catechol APAP metabolites originating from another phase I oxidation pathway (i.e., 3-OH-APAP and 3-OCH_3-APAP present as non-conjugated and conjugated forms).

Of the 15 metabolites, we also annotated conjugated forms of S-methyl-3-thioacetaminophen (S-CH_3-APAP-S and S-CH_3-APAP-Glu) and S-methyl-3-thioacetaminophen sulphoxide (SO-CH_3-APAP-S and SO-CH_3-APAP-Glu) up to now unreported in humans as conjugated. These 4 metabolites had previously only been reported in rodents (rat and hamster) and dogs (albeit non-conjugated in case of SO-CH_3-APAP-S and SO-CH_3-APAP-Glu; i.e., SO-CH_3-APAP) (Gemborys and Mudge, 1981; Hart et al., 1982; Mikov et al., 1988). The two metabolites NAC-O-APAP and SH-APAP-Glu have not at all been detected before in any species to the best of our knowledge. Except for NAC-O-APAP, these conjugated thiomethyl metabolites (i.e., S-CH_3-APAP-S, S-CH_3-APAP-Glu, SO-CH_3-APAP-S and SO-CH_3-APAP-Glu metabolites) were mainly detected in samples collected *+1-2 days* after APAP intake.

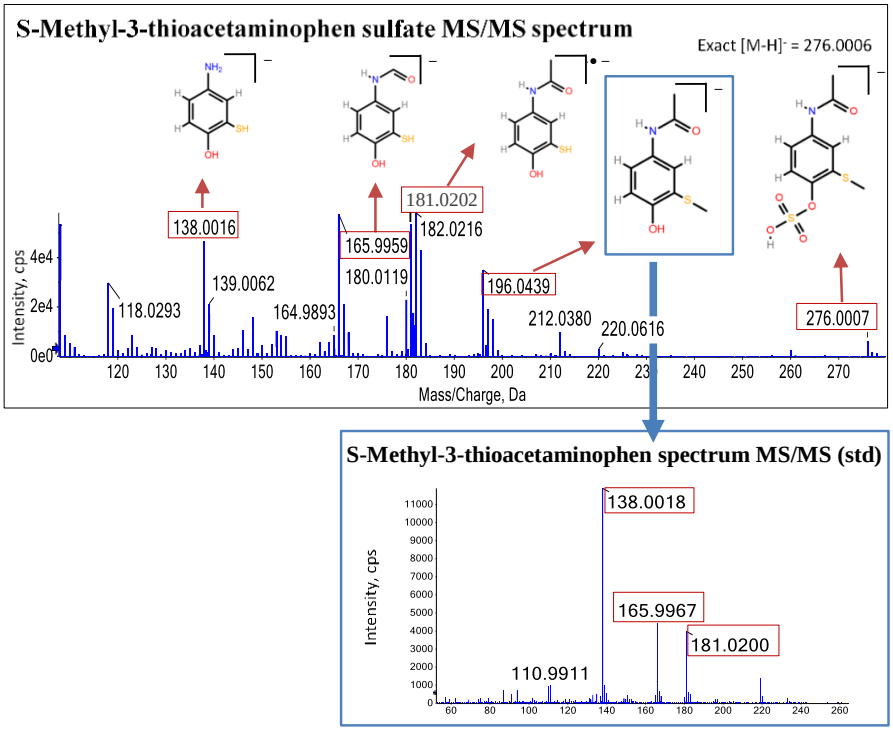

Fig.2. Experimental MS/MS spectrum of *S*-Methyl-3-thioacetaminophen sulfate from a urine sample (+24h time point) after APAP exposure and MS/MS spectrum of the standard of *S*-Methyl-3-thioacetaminophen. MS/MS mass fragmentation information was obtained in SWATH mode using an UHPLC-ESI-QTOF-MS in –ESI mode. *In silico* fragmentation software (i.e., MetFrag and CFM-ID) were utilized for computer assisted identification for *S*-Methyl-3-thioacetaminophen sulfate. Further confirmation of experimental MS/MS fragments could be obtained by injecting the commercially available standard of S-CH_3-APAP.

In silico fragmentation software such as MetFrag (Ruttkies et al., 2016) and CFM-ID (Djoumbou-Feunang et al., 2019) were utilized for computer assisted annotation of S-CH_3-APAP-S and SO-CH_3-APAP-S since many potential candidates were matching the matching the accurate mass of these marker ions within PubChem (e.g., 1337 candidates for m/z=276.004 in –ESI mode $[M-H]^-$; 5 ppm mass tolerance). Further confirmation of the S-CH_3-APAP-S annotation were obtained by comparing its experimental MS/MS fragments with those of its non-conjugated form (S-CH_3-APAP), which was obtained by injecting the S-CH_3-APAP standard in SWATH mode (Fig. 2). Moreover, the MS/MS fragments of S-CH_3-APAP-S we report are matching those observed experimentally in mice after APAP exposure (Patterson et al., 2013). The other marker with an *m/z* of 291.9945 in –ESI mode ($[M-H]^-$) could be annotated as S-CH_3-APAP sulfoxide derivative, i.e., SO-CH_3-APAP-S. Although standards or MS/MS spectra are currently unavailable for most of these metabolites, a high level of confidence could be reached (Schymanski et al., 2014; Sumner et al., 2007) given that a match was observed with the MS/MS profile of the standard for the unconjugated S-CH_3-APAP and that the metabolites are related to the same pathway of elimination of thio metabolites.

Relevance of thiomethyl metabolites for monitoring APAP pharmaceutical use

To understand the relevance of the 4 conjugated thiomethyl metabolites (S-CH_3-APAP-S, S-CH_3-APAP-Glu, SO-CH_3-APAP-S and SO-CH_3-APAP-Glu) and the two previously unreported metabolites NAC-O-APAP and SH-APAP-Glu metabolites to improve human biomonitoring of APAP , we next investigated the relative contributions of APAP metabolites in urine and plasma based on their analytical responses (normalized peak areas) for each time point. We also compared the analytical responses of free APAP and its phase II conjugates, conventionally used in standard APAP biomonitoring methods, to those of catechol and glutathione-derived APAP metabolites. Although these HRMS-based data are not representative of the importance of each metabolite in APAP metabolism in terms of quantity excreted, they do provide valuable information regarding the most sensitive metabolites (in respect to their ionization efficiency) to be used for optimizing APAP monitoring in humans. The relative contributions based on normalized peak area of APAP metabolites are presented in Fig.3 for both blood and urine.

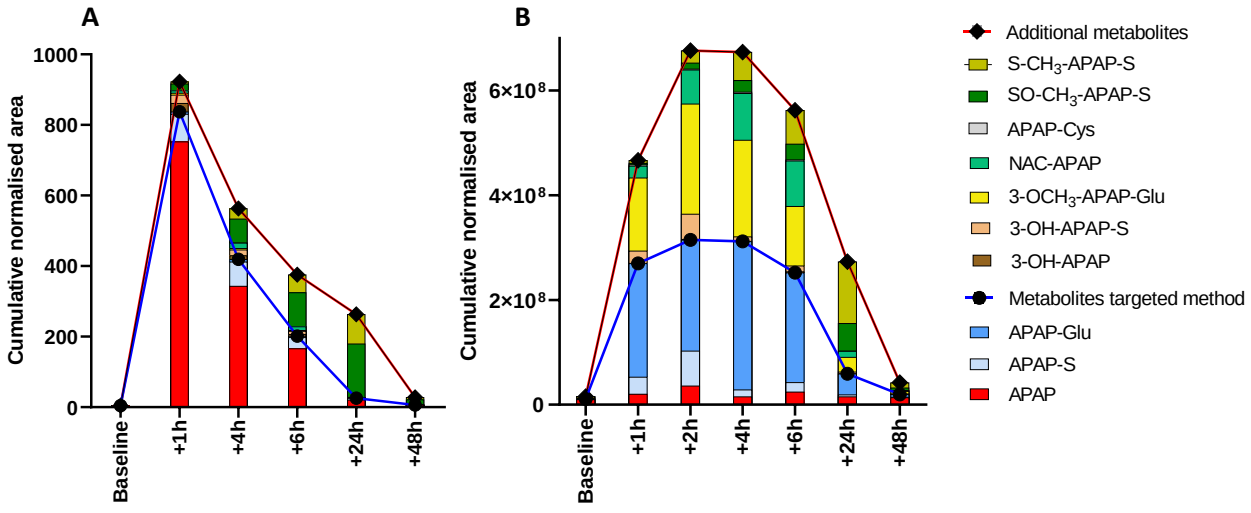

Fig. 3. Analytical responses (represented as cumulative normalised peak areas) of APAP metabolites classically used for targeted methods (i.e., free APAP, APAP-Glu and APAP-S) and the other metabolites detected using the non-targeted analyses in blood (A) and urine (B). APAP and its metabolites were manually re-integrated using the Sciex OS Analytics tool. The integrated peak area of individual markers was normalized to APAP-d4 for plasma or with a corrective factor based on the total peak area for urine.

Of the 6 metabolites previously unreported in humans, only the sulfate thiomethyl metabolites (i.e. S-CH_3-APAP-S and SO-CH_3-APAP-S) present significant analytical responses and therefore potential to improve APAP monitoring. Relative contributions of S-CH_3-APAP-Glu, SO-CH_3-APAP-Glu, NAC-O-APAP and SH-APAP-Glu are not reported on Fig. 3 as they were <1% for all time points after APAP intake. In particular, we observed that S-CH_3-APAP-S and SO-CH_3-APAP-S are major metabolites for the 24h and 48h time points in blood and urine while the contributions of these S-CH_3-APAP-S and SO-CH_3-APAP-S metabolites are minor before APAP intake (baseline).

More specifically, the relative contribution of the parent APAP was major in blood for the first time points after APAP intake (relative contribution of 44-82% before 24h) while these of other APAP metabolites such as phase II APAP-S, catechol APAP (OH-APAP and OH-APAP-S), or NAC-APAP were all comprised below 12% for the same time points. Relative contributions of S-CH_3-APAP-S and SO-CH_3-APAP-S increased overtime after APAP intake, finally becoming dominant for the 24h and 48h time points (i.e., 90% and 78% at 24h and 48h, respectively, for the sum of both metabolites).

In urine, the metabolites conventionally used for the monitoring of APAP using targeted approach, i.e. free APAP and the phase II conjugates (APAP-S and APAP-Glu) contributed to 45-58% of the analytical response for the time points comprised between +1h and 6h. APAP-Glu was the major metabolite for these time points (relative contribution of 31-46% overall). The other catechol or glutathione-derived metabolites and conjugated thiomethyl metabolites contributed altogether to the remaining 42-55% of the analytical response from 1h up to 6h after APAP intake. For these 1-6h time points, 3-OCH_3-APAP-Glu was the major metabolite among these metabolites (relative contribution of 20-31% overall), followed by NAC-APAP (5-15 % overall), S-CH_3-APAP-S (1-11% overall) and SO-CH_3-APAP-S (0.6 -5% overall). As observed in blood, S-CH_3-APAP-S and SO-CH_3-APAP-S were major metabolites for the 24h and 48h time points (relative contribution for the sum of both metabolites of 36-62% between 24h and 48h).

As mentioned earlier, the relative contributions of APAP metabolites reported here are not fully representative of the importance of each metabolite in APAP metabolism in terms of quantity excreted. APAP is known to be extensively metabolized in the liver and based on literature reviews on APAP pharmacokinetics, it is often considered that free APAP and direct phase II conjugates represent between 65-85% of the quantity excreted (mainly as APAP-Glu) while the other catechol and glutathione-derived metabolites can represent up to 20% together of the quantity excreted (Bessems and Vermeulen, 2001; Mazaleuskaya et al., 2015). However, based on the high analytical response we observed here for the conjugated catechol 3-OCH3-APAP-Glu, we show that this metabolite would be a good candidate to improve the analytical sensitivity of targeted methods based on LC-ESI-MS/MS, which is the standard platform used for APAP monitoring.

Background APAP exposure levels did not seem to be accompanied by significant amounts of the conjugated thiomethyl metabolites, while after pharmaceutical use (high exposure) scenario, they could be determined sensitively more than 48h post exposure, suggesting that S-CH_3-APAP-S and SO-CH_3-APAP-S have great potential to retrospectively assess pharmaceutical use of APAP in humans.

The conjugated thiomethyl metabolites and the thiomethyl shunt pathway

We next studied the kinetics of formation of individual metabolites by comparing their normalized abundance in plasma and urine for each time point before and after APAP intake. The kinetics of formation of free APAP, phase II metabolites (APAP-Glu and APAP-S), catechol metabolites (3-OCH3-APAP-Glu, OH-APAP-S and OH-APAP), glutathione derived metabolites (NAC-APAP and Cyst-APAP) and thiomethyl metabolites (S-CH3-APAP-S and SO-CH3-APAP-S) in both blood and urine are presented in Fig. 4.

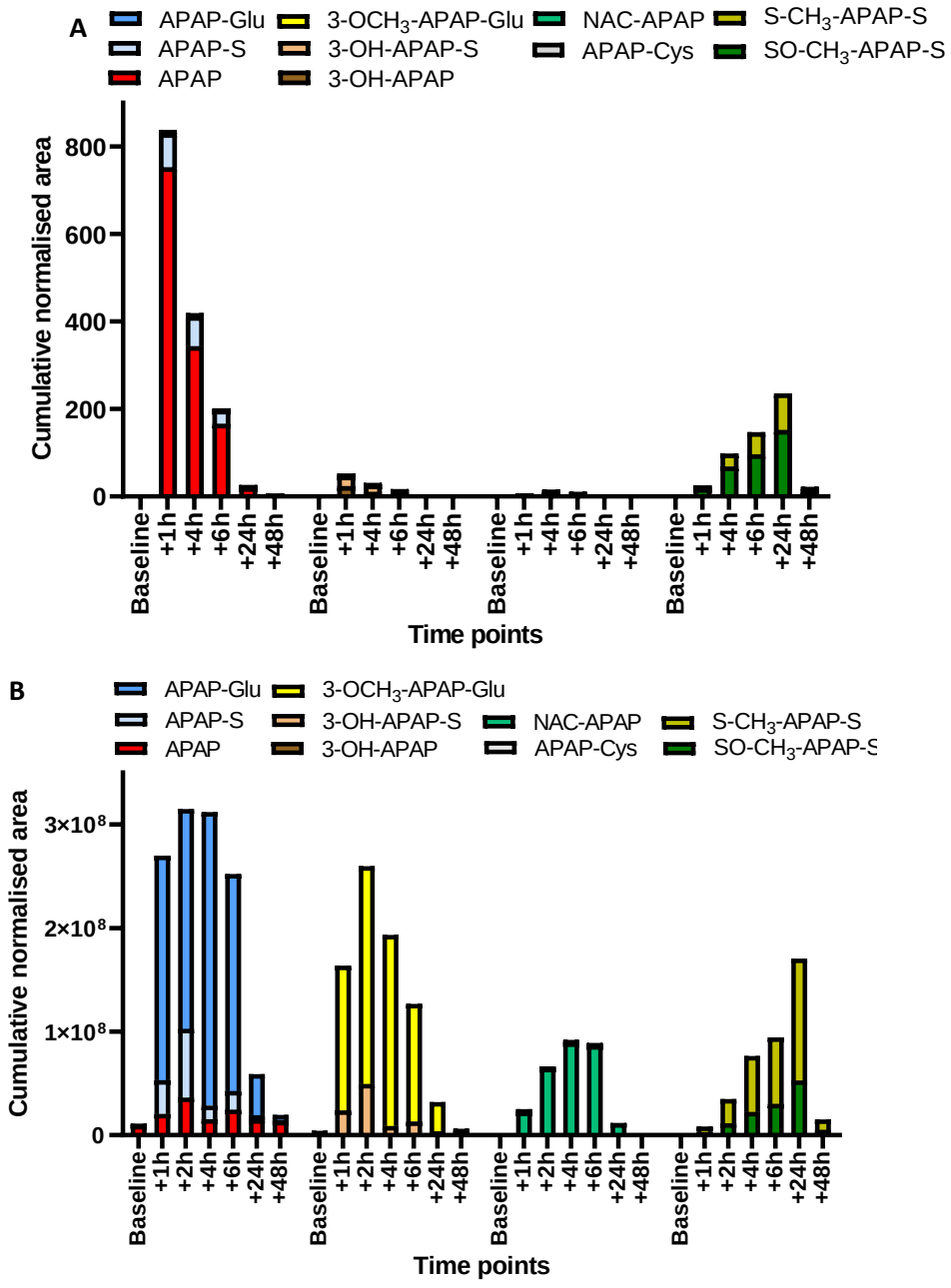

Fig. 4. Kinetics of formation of free APAP, phase II metabolites (APAP-Glu and APAP-S), catechol metabolites (3-OCH_3-APAP-Glu, OH-APAP-S and OH-APAP), glutathione derived metabolites (NAC-APAP and APAP-Cys) and thiomethyl metabolites (S-CH_3-APAP-S and SO-CH_3-APAP-S) detected using the non-targeted screening based on UHPLC-ESI-QTOF-MS analyses in **(A)** blood plasma and **(B)** urine before intake and at different time points after intake. No significant shift (i.e. below 20%) in analytical sensitivity was observed during the batch to make this time point comparison for individual metabolites. APAP and its metabolites were manually re-integrated using the Sciex OS Analytics tool. The integrated peak area of individual markers was normalized to APAP-d4 for plasma or with a corrective factor based on the total peak area for urine.

Similarly to the results obtained with the targeted methods, we observed that APAP was absorbed quickly in the blood and reached the peak blood concentrations within 60 minutes after ingestion, as previously observed (Mazaleuskaya et al., 2015). The APAP signal had decreased to less than 50% 4h after intake before reaching basal levels after 24-48h. Similar kinetics of formation were observed in blood for the minor APAP catechol metabolites (peak time at 1h) while NAC-APAP peaked at 4h instead, which could be explained by the fact that NAC-APAP is formed after a higher number of

successive reactions involving phase I reactions, glutathione conjugation and enzyme reactions from the mercapturic acid pathway. Interestingly, S-CH3-APAP-S and SO-CH3-APAP-S metabolites in general showed delayed appearance with a peak time at 24h in blood plasma.

In urine, free APAP, phase II metabolites (APAP-Glu and APAP-S) and catechol metabolites (3-OCH3-APAP-Glu, OH-APAP-S and OH-APAP), peaked at 2h. This is different from the targeted results that showed that "total APAP" measured as free APAP, APAP-Glu and APAP-S after enzymatic conjugation peaked at 4h in urine instead. However, direct comparison of quantitative data from targeted methods and semi-quantitative data from HRMS-based methods can be difficult because of the lack of specific correction with proper labelled internal standards. NAC-APAP peaked after the direct phase II conjugates and the catechol metabolites (peak time is at 4h), probably because of the higher number of successive reactions to form the mercapturic acid as mentioned earlier. Like in blood, S-CH3-APAP-S and SO-CH3-APAP-S metabolites in general showed delayed appearance compared with direct phase II conjugates, catechol metabolites and glutathione-derived metabolites that peaked in the 1h-4h window.

This delayed appearance suggests that the formation of S-CH_3-APAP-S and SO-CH_3-APAP-S was limited by prior biological steps as opposed to the direct excretion for other metabolites. A similar lag time has been observed in enterohepatic circulation due to the intestinal transit period of metabolites to sites of biotransformation (Roberts et al., 2002). Moreover, the biotransformation that leads to the formation of thiomethyl metabolites have been shown to occur in rodents via the enterohepatic circulation and biliary excretion of the glutathione-derived conjugates (i.e., APAP-Cys and NAC-APAP) into the intestine with subsequent microbiotic transformation (Gemborys and Mudge, 1981) (Fig. 5). This transformation includes activity of the cysteine S-conjugate β-lyase and subsequent methylation involving an active form of methionine (Cooper et al., 2011; Gemborys and Mudge, 1981). Therefore, our data strongly suggests that a thiomethyl shunt pathway (Cooper et al., 2011) that results in formation of the thiomethyl metabolites is also present in humans. In agreement with that, the cysteine conjugate beta-lyase was already previously detected in a majority of gastrointestinal bacteria tested (Larsen, 1985).

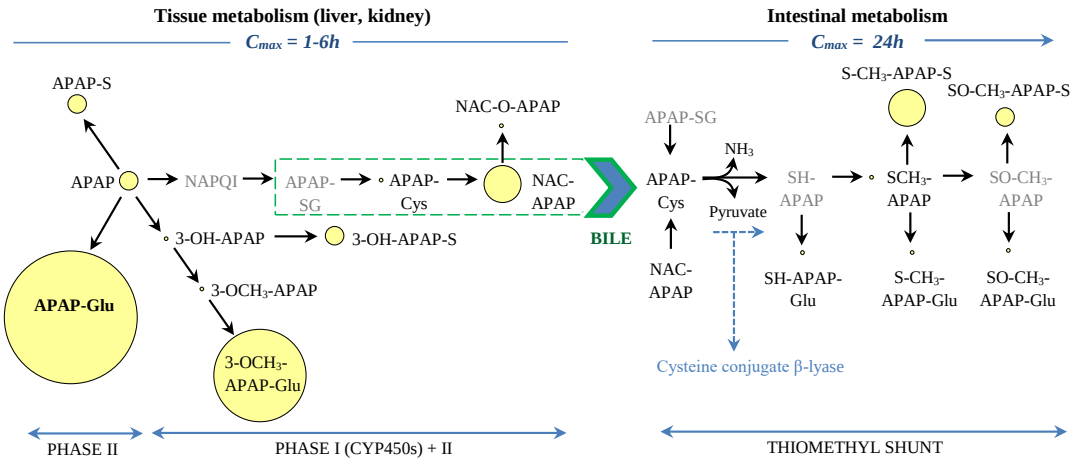

Fig. 5. Revisited APAP metabolism in human including the thiomethyl shunt and the role of cysteine conjugate beta-lyase from the non-targeted screening results. APAP metabolites in grey are known precursors but not detected during this experiment because of their lability or lower levels.

Hence, our results show that the conjugated thiomethyl metabolites S-CH_3-APAP-S and SO-CH_3-APAP-S have the potential to improve APAP biomonitoring in humans since their delayed elimination peaks

could extend the window of exposure and thus potentially decrease underestimation or misclassification in epidemiological studies when sampling is performed >24h after intake.

Conclusion

Reliable biomonitoring methods are essential for proper risk assessment. Estimations of exposure in most existing epidemiological data of APAP have limitations due to potential recall bias or reliance on standard analytical methods for exposure assessment which include metabolites that capture only partially the exposure and/or are too rapidly eliminated. Our data provide a proof-of-concept for HRMS-based non-targeted analyses as a valuable addition to the tool set for the identification of metabolites suitable as exposure biomarkers, complementing HRMS-based suspect screening approaches (e.g., (Lessmann et al., 2018)) and traditional approaches (e.g.,(Bury et al., 2019)), and thus contributing to the optimization of current standard methods. The findings based on non-targeted analyses after APAP intake suggest that thiomethyl sulfate APAP metabolites and 3-OCH_3-APAP-Glu should be included in future biomonitoring methods for several reasons. First, the conjugated thiomethyl metabolites have later peak levels and therefore extend the window of exposure decreasing underestimation. Secondly, the data suggest that they provide biomarkers of comparable sensitivity as free APAP and its phase II conjugates. Thirdly, the thiomethyl sulfate APAP metabolites provide information regarding metabolic pathways worth of interest from a toxicological point of view since they are derived from the toxic NAPQI metabolites.

We acknowledge that non-targeted analyses present limitations inherent to the production of semi-quantitative data and therefore the estimates we provide here will require further evaluation based on quantitative measurements and authentic standards. Nevertheless, our quality control data, showing no drift in analytical sensitivity during our batch analyses, provide confidence for the sample to sample comparison made to study the kinetics of appearance of individual metabolites at different time points. The comparison of the relative contributions of APAP metabolites based on their analytical responses is relevant to determine which metabolites can be used to optimize standard targeted methods given that similar platforms (LC-MS) and ion sources (i.e. electrospray ion sources) are utilized for the APAP targeted approach. The standard APAP biomonitoring methods include a deconjugation step using glucuronidases and sulfates. Hence, standard APAP biomonitoring methods could already be upgraded by including 3-OCH3-APAP and S-CH3-APAP metabolites as these standards are already commercially available. We therefore believe that the limitations in quantitative information value should not overshadow the importance of the identification of the thiomethyl conjugates and their potential to improve the monitoring of non-persistent chemicals such as APAP.

The role of the mercapturate pathway and the cysteine *S*-conjugate beta-lyases in the metabolism of drugs (e.g., methazolamide, cisplatin) have been already demonstrated in mammalians (Cooper et al., 2011). Furthermore, the cysteine *S*-conjugate beta-lyases can play an important key role in the bioactivation of halogenated alkenes (some of which are environmental contaminants produced on an industrial scale), and if the sulfur-containing fragment is reactive, the parent cysteine S-conjugate may be toxic, particularly to kidney mitochondria (Cooper et al., 2011; Cooper and Pinto, 2006). Despite its biological importance, there are surprisingly few data regarding identities of xenobiotics detoxified using the mercapturate and thiomethyl shunt pathway. Determining to which extent this happens could improve biomonitoring analytical methods by including more relevant metabolites and thus reduce potential serious underestimations for the reason stated above for APAP. This effort will require a coordinated approach between experts working with both targeted and untargeted approaches and the synthesis of standards for individual chemicals and their metabolites for accurate measurements. Analytical methods based on HRMS are still under development and are not mature enough to replace targeted methods in large biomonitoring programs where accurate quantitative data are needed. However, we advocate for their use as discovery-based approach, as demonstrated here, to update targeted methods with the best metabolites in order to provide the most

comprehensive view of the exposure for proper risk assessment for APAP and other similar non-persistent chemicals.

Author's contribution

AD contributed to the study design, data collection, data analysis, data interpretation, figures and tables editing, drafting and text revision; JC contributed to the data collection, data analysis, figures and tables editing, text revision; TL contributed to the data analysis, text revision, RAS contributed to the data collection, data analysis, text revision, MDD contributed to the study design, sample collection, text revision, HMK contributed to data analysis, data interpretation, figures and tables editing, drafting and text revision, DB contributed to data collection, data analysis, data interpretation, and text revision, BJ contributed to figures and tables editing, drafting and text revision, DMK contributed to the study design, data collection, data analysis, data interpretation, figures and tables editing, drafting and text revision.

Acknowledgment

We declare no competing interests. We thank Shanna Swan for her editorial comments and Romain Letourneur and Claudia Pälmke for technical assistance. The study was supported by the Candys Foundation and a research chair of excellence (2016-52/IdeX University of Sorbonne Paris Cité) awarded to AD.

Reference

Adusumilli, R., Mallick, P., 2017. Data Conversion with ProteoWizard msConvert. Methods Mol Biol. 1550, 339-368.

Albert, O., Desdoits-Lethimonier, C., Lesne, L., Legrand, A., Guille, F., Bensalah, K., Dejucq-Rainsford, N., Jegou, B., 2013. Paracetamol, aspirin and indomethacin display endocrine disrupting properties in the adult human testis in vitro. Hum Reprod. 28, 1890-8.

Bessems, J.G., Vermeulen, N.P., 2001. Paracetamol (acetaminophen)-induced toxicity: molecular and biochemical mechanisms, analogues and protective approaches. Crit Rev Toxicol. 31, 55-138.

Bornehag, C.G., Reichenberg, A., Hallerback, M.U., Wikstrom, S., Koch, H.M., Jonsson, B.A., Swan, S.H., 2018. Prenatal exposure to acetaminophen and children's language development at 30 months. Eur Psychiatry. 51, 98-103.

Bury, D., Modick-Biermann, H., Leibold, E., Brüning, T., Koch, H.M., 2019. Urinary metabolites of the UV filter octocrylene in humans as biomarkers of exposure. Arch Toxicol. 93, 1227-1238.

Chetwynd, A.J., Abdul-Sada, A., Hill, E.M., 2015. Solid-phase extraction and nanoflow liquid chromatography-nanoelectrospray ionization mass spectrometry for improved global urine metabolomics. Anal Chem. 87, 1158-65.

Cooper, A.J., Krasnikov, B.F., Niatsetskaya, Z.V., Pinto, J.T., Callery, P.S., Villar, M.T., Artigues, A., Bruschi, S.A., 2011. Cysteine S-conjugate beta-lyases: important roles in the metabolism of naturally occurring sulfur and selenium-containing compounds, xenobiotics and anticancer agents. Amino Acids. 41, 7-27.

Cooper, A.J., Pinto, J.T., 2006. Cysteine S-conjugate beta-lyases. Amino Acids. 30, 1-15.

David, A., Abdul-Sada, A., Lange, A., Tyler, C.R., Hill, E.M., 2014. A new approach for plasma (xeno)metabolomics based on solid-phase extraction and nanoflow liquid chromatography-nanoelectrospray ionisation mass spectrometry. J Chromatogr A. 1365, 72-85.

David, A., Lange, A., Abdul-Sada, A., Tyler, C.R., Hill, E.M., 2017. Disruption of the Prostaglandin Metabolome and Characterization of the Pharmaceutical Exposome in Fish Exposed to Wastewater Treatment Works Effluent As Revealed by Nanoflow-Nanospray Mass Spectrometry-Based Metabolomics. Environ Sci Technol. 51, 616-624.

Djoumbou-Feunang, Y., Pon, A., Karu, N., Zheng, J., Li, C., Arndt, D., Gautam, M., Allen, F., Wishart, D.S., 2019. CFM-ID 3.0: Significantly Improved ESI-MS/MS Prediction and Compound Identification. Metabolites. 9, 72.

Ferri, F.F., 2016. Ferri's clinical advisor 2017: 5 Books in 1. Elsevier Health Sciences : 1154–1155 ISBN 9780323448383.
Gemborys, M.W., Mudge, G.H., 1981. Formation and disposition of the minor metabolites of acetaminophen in the hamster. Drug Metab Dispos. 9, 340-51.
Guijas, C., Montenegro-Burke, J.R., Domingo-Almenara, X., Palermo, A., Warth, B., Hermann, G., Koellensperger, G., Huan, T., Uritboonthai, W., Aisporna, A.E., Wolan, D.W., Spilker, M.E., Benton, H.P., Siuzdak, G., 2018. METLIN: A Technology Platform for Identifying Knowns and Unknowns. Anal Chem. 90, 3156-3164.
Hanna, P.E., Anders, M.W., 2019. The mercapturic acid pathway. Crit Rev Toxicol. 49, 819-929.
Hart, S.J., Healey, K., Smail, M.C., Calder, I.C., 1982. 3-thiomethylparacetamol sulphate and glucuronide: metabolites of paracetamol and N-hydroxyparacetamol. Xenobiotica. 12, 381-6.
Horai, H., Arita, M., Kanaya, S., Nihei, Y., Ikeda, T., Suwa, K., Ojima, Y., Tanaka, K., Tanaka, S., Aoshima, K., Oda, Y., Kakazu, Y., Kusano, M., Tohge, T., Matsuda, F., Sawada, Y., Hirai, M.Y., Nakanishi, H., Ikeda, K., Akimoto, N., Maoka, T., Takahashi, H., Ara, T., Sakurai, N., Suzuki, H., Shibata, D., Neumann, S., Iida, T., Tanaka, K., Funatsu, K., Matsuura, F., Soga, T., Taguchi, R., Saito, K., Nishioka, T., 2010. MassBank: a public repository for sharing mass spectral data for life sciences. J Mass Spectrom. 45, 703-14.
Hurwitz, J., Sands, S., Davis, E., Nielsen, J., Warholak, T., 2014. Patient knowledge and use of acetaminophen in over-the-counter medications. J Am Pharm Assoc (2003). 54, 19-26.
Kanehisa, M., 2002. The KEGG database. Novartis Found Symp. 247, 91-101; discussion 101-3, 119-28, 244-52.
Kim, S., Chen, J., Cheng, T., Gindulyte, A., He, J., He, S., Li, Q., Shoemaker, B.A., Thiessen, P.A., Yu, B., Zaslavsky, L., Zhang, J., Bolton, E.E., 2019. PubChem 2019 update: improved access to chemical data. Nucleic Acids Res. 47, D1102-d1109.
Konkel, L., 2018. Reproductive Headache? Investigating Acetaminophen as a Potential Endocrine Disruptor. Environ Health Perspect. 126, 032001.
Kortenkamp, A., 2020. Which chemicals should be grouped together for mixture risk assessments of male reproductive disorders? Mol Cell Endocrinol. 499, 110581.
Kortenkamp, A., Koch, H.M., 2020. Refined reference doses and new procedures for phthalate mixture risk assessment focused on male developmental toxicity. International Journal of Hygiene and Environmental Health. 224, 113428.
Kristensen, D.M., Desdoits-Lethimonier, C., Mackey, A.L., Dalgaard, M.D., De Masi, F., Munkbol, C.H., Styrishave, B., Antignac, J.P., Le Bizec, B., Platel, C., Hay-Schmidt, A., Jensen, T.K., Lesne, L., Mazaud-Guittot, S., Kristiansen, K., Brunak, S., Kjaer, M., Juul, A., Jegou, B., 2018. Ibuprofen alters human testicular physiology to produce a state of compensated hypogonadism. Proc Natl Acad Sci U S A. 115, E715-E724.
Kristensen, D.M., Lesne, L., Le Fol, V., Desdoits-Lethimonier, C., Dejucq-Rainsford, N., Leffers, H., Jegou, B., 2012. Paracetamol (acetaminophen), aspirin (acetylsalicylic acid) and indomethacin are anti-androgenic in the rat foetal testis. Int J Androl. 35, 377-84.
Kristensen, D.M., Mazaud-Guittot, S., Gaudriault, P., Lesne, L., Serrano, T., Main, K.M., Jegou, B., 2016. Analgesic use - prevalence, biomonitoring and endocrine and reproductive effects. Nat Rev Endocrinol. 12, 381-93.
Larsen, G.L., 1985. Distribution of cysteine conjugate beta-lyase in gastrointestinal bacteria and in the environment. Xenobiotica. 15, 199-209.
Lessmann, F., Bury, D., Weiss, T., Hayen, H., Brüning, T., Koch, H.M., 2018. De-novo identification of specific exposure biomarkers of the alternative plasticizer di(2-ethylhexyl) terephthalate (DEHTP) after low oral dosage to male volunteers by HPLC-Q-Orbitrap-MS. Biomarkers. 23, 196-206.
Mazaleuskaya, L.L., Sangkuhl, K., Thorn, C.F., FitzGerald, G.A., Altman, R.B., Klein, T.E., 2015. PharmGKB summary: pathways of acetaminophen metabolism at the therapeutic versus toxic doses. Pharmacogenetics and genomics. 25, 416-426.

Mikov, M., Caldwell, J., Dolphin, C.T., Smith, R.L., 1988. The role of intestinal microflora in the formation of the methylthio adduct metabolites of paracetamol. Studies in neomycin-pretreated and germ-free mice. Biochem Pharmacol. 37, 1445-9.
Modick, H., Schütze, A., Pälmke, C., Weiss, T., Brüning, T., Koch, H.M., 2013. Rapid determination of N-acetyl-4-aminophenol (paracetamol) in urine by tandem mass spectrometry coupled with on-line clean-up by two dimensional turbulent flow/reversed phase liquid chromatography. Journal of Chromatography B. 925, 33-39.
Modick, H., Weiss, T., Dierkes, G., Bruning, T., Koch, H.M., 2014. Ubiquitous presence of paracetamol in human urine: sources and implications. Reproduction. 147, R105-17.
Modick, H., Weiss, T., Dierkes, G., Koslitz, S., Kafferlein, H.U., Bruning, T., Koch, H.M., 2016. Human metabolism and excretion kinetics of aniline after a single oral dose. Arch Toxicol. 90, 1325-33.
Nielsen, J.K., Modick, H., Morck, T.A., Jensen, J.F., Nielsen, F., Koch, H.M., Knudsen, L.E., 2015. N-acetyl-4-aminophenol (paracetamol) in urine samples of 6-11-year-old Danish school children and their mothers. Int J Hyg Environ Health. 218, 28-33.
Patterson, A.D., Carlson, B.A., Li, F., Bonzo, J.A., Yoo, M.H., Krausz, K.W., Conrad, M., Chen, C., Gonzalez, F.J., Hatfield, D.L., 2013. Disruption of thioredoxin reductase 1 protects mice from acute acetaminophen-induced hepatotoxicity through enhanced NRF2 activity. Chem Res Toxicol. 26, 1088-96.
Pence, H.E., Williams, A., 2010. ChemSpider: An Online Chemical Information Resource. Journal of Chemical Education. 87, 1123-1124.
Roberts, M.S., Magnusson, B.M., Burczynski, F.J., Weiss, M., 2002. Enterohepatic Circulation. Clinical Pharmacokinetics. 41, 751-790.
Rohart, F., Gautier, B., Singh, A., KA, L.C., 2017. mixOmics: An R package for 'omics feature selection and multiple data integration. PLoS Comput Biol. 13, e1005752.
Ruttkies, C., Schymanski, E.L., Wolf, S., Hollender, J., Neumann, S., 2016. MetFrag relaunched: incorporating strategies beyond in silico fragmentation. Journal of cheminformatics. 8, 3-3.
Schulz, M., Iwersen-Bergmann, S., Andresen, H., Schmoldt, A., 2012. Therapeutic and toxic blood concentrations of nearly 1,000 drugs and other xenobiotics. Crit Care. 16, R136.
Schymanski, E.L., Jeon, J., Gulde, R., Fenner, K., Ruff, M., Singer, H.P., Hollender, J., 2014. Identifying small molecules via high resolution mass spectrometry: communicating confidence. Environ Sci Technol. 48, 2097-8.
Smith, C.A., Want, E.J., O'Maille, G., Abagyan, R., Siuzdak, G., 2006. XCMS: processing mass spectrometry data for metabolite profiling using nonlinear peak alignment, matching, and identification. Anal Chem. 78, 779-87.
Sumner, L.W., Amberg, A., Barrett, D., Beale, M.H., Beger, R., Daykin, C.A., Fan, T.W., Fiehn, O., Goodacre, R., Griffin, J.L., Hankemeier, T., Hardy, N., Harnly, J., Higashi, R., Kopka, J., Lane, A.N., Lindon, J.C., Marriott, P., Nicholls, A.W., Reily, M.D., Thaden, J.J., Viant, M.R., 2007. Proposed minimum reporting standards for chemical analysis Chemical Analysis Working Group (CAWG) Metabolomics Standards Initiative (MSI). Metabolomics. 3, 211-221.
Want, E.J., Wilson, I.D., Gika, H., Theodoridis, G., Plumb, R.S., Shockcor, J., Holmes, E., Nicholson, J.K., 2010. Global metabolic profiling procedures for urine using UPLC–MS. Nature Protocols. 5, 1005.
Wishart, D., Arndt, D., Pon, A., Sajed, T., Guo, A.C., Djoumbou, Y., Knox, C., Wilson, M., Liang, Y., Grant, J., Liu, Y., Goldansaz, S.A., Rappaport, S.M., 2015. T3DB: the toxic exposome database. Nucleic Acids Res. 43, D928-34.
Wishart, D.S., Feunang, Y.D., Guo, A.C., Lo, E.J., Marcu, A., Grant, J.R., Sajed, T., Johnson, D., Li, C., Sayeeda, Z., Assempour, N., Iynkkaran, I., Liu, Y., Maciejewski, A., Gale, N., Wilson, A., Chin, L., Cummings, R., Le, D., Pon, A., Knox, C., Wilson, M., 2018a. DrugBank 5.0: a major update to the DrugBank database for 2018. Nucleic Acids Res. 46, D1074-d1082.
Wishart, D.S., Feunang, Y.D., Marcu, A., Guo, A.C., Liang, K., Vázquez-Fresno, R., Sajed, T., Johnson, D., Li, C., Karu, N., Sayeeda, Z., Lo, E., Assempour, N., Berjanskii, M., Singhal, S., Arndt, D.,

Liang, Y., Badran, H., Grant, J., Serra-Cayuela, A., Liu, Y., Mandal, R., Neveu, V., Pon, A., Knox, C., Wilson, M., Manach, C., Scalbert, A., 2018b. HMDB 4.0: the human metabolome database for 2018. Nucleic Acids Res. 46, D608-d617.

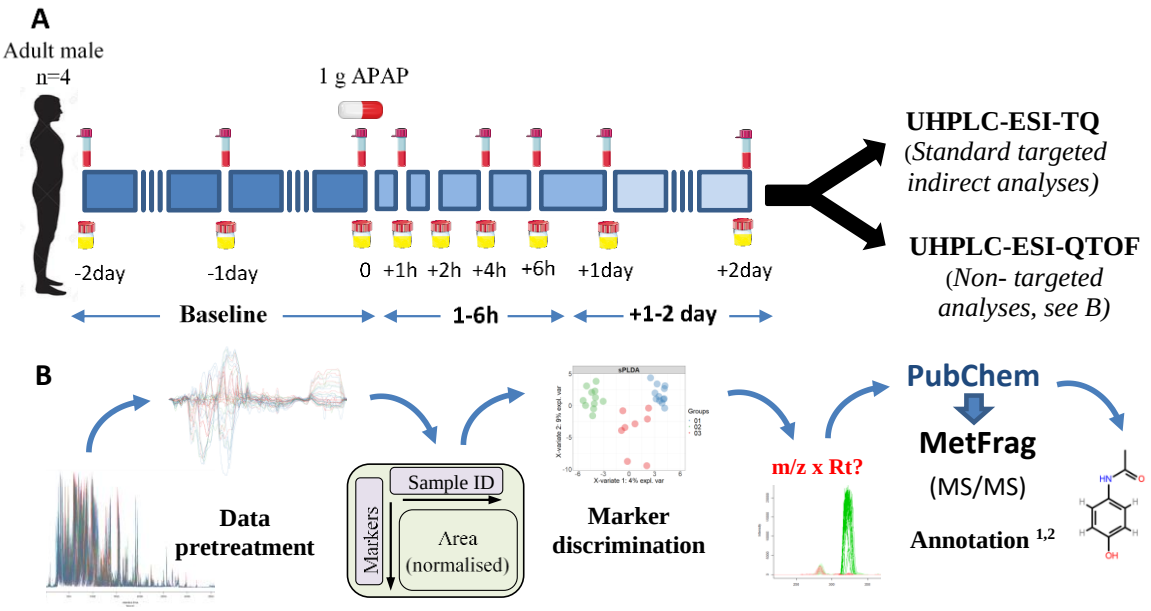

Figure S1. **Design of the longitudinal *in vivo* study using four adult volunteers (men) over four days with an administration of 1 gram of APAP on the third day (A) and visualization of the main steps involved for the non-targeted workflow (B).** [1] (Sumner et al., 2007), [2] (Schymanski et al., 2014)

Figure S2. **Non-supervised principal component analysis scores plot of the chemical profiles of blood plasma of adult males (n=4, person 1 to 4) before and after administration of 1 g paracetamol.**
The samples were profiled in negative mode (A) and positive (B) modes by UHPLC-ESI-TOF-MS. Composite quality control (QC, n=6) samples (diluted 2-fold because of the very low reconstitution volume) were used to monitor the analytical performance of the MS platform. **1:** *baseline group* = samples collected two days and just prior to intake of APAP (n=12), **2:** *1-6h group* = samples collected +1, +4, +6 hours after intake (n=11) and **3:** *+1-2 days group* = samples collected in the morning the subsequent two days (n=8).

Figure S2. **Non-supervised principal component analysis scores plot of the chemical profiles of urine of adult males (n=4, person 1 to 4) before and after administration of 1 g paracetamol.**
The samples were profiled in negative mode (A) and positive (B) modes by UHPLC-ESI-TOF-MS. Composite quality control (QC, n=9) samples (diluted 2-fold because of the very low reconstitution volume) were used to monitor the analytical performance of the MS platform. **1:** *baseline group* = samples collected two days and just prior to intake of APAP (n=12), **2:** *1-6h group* = samples collected +1, +2, +4, +6 hours after intake (n=15) and **3:** *+1-2 days group* = samples collected in the morning the subsequent two days (n=8).

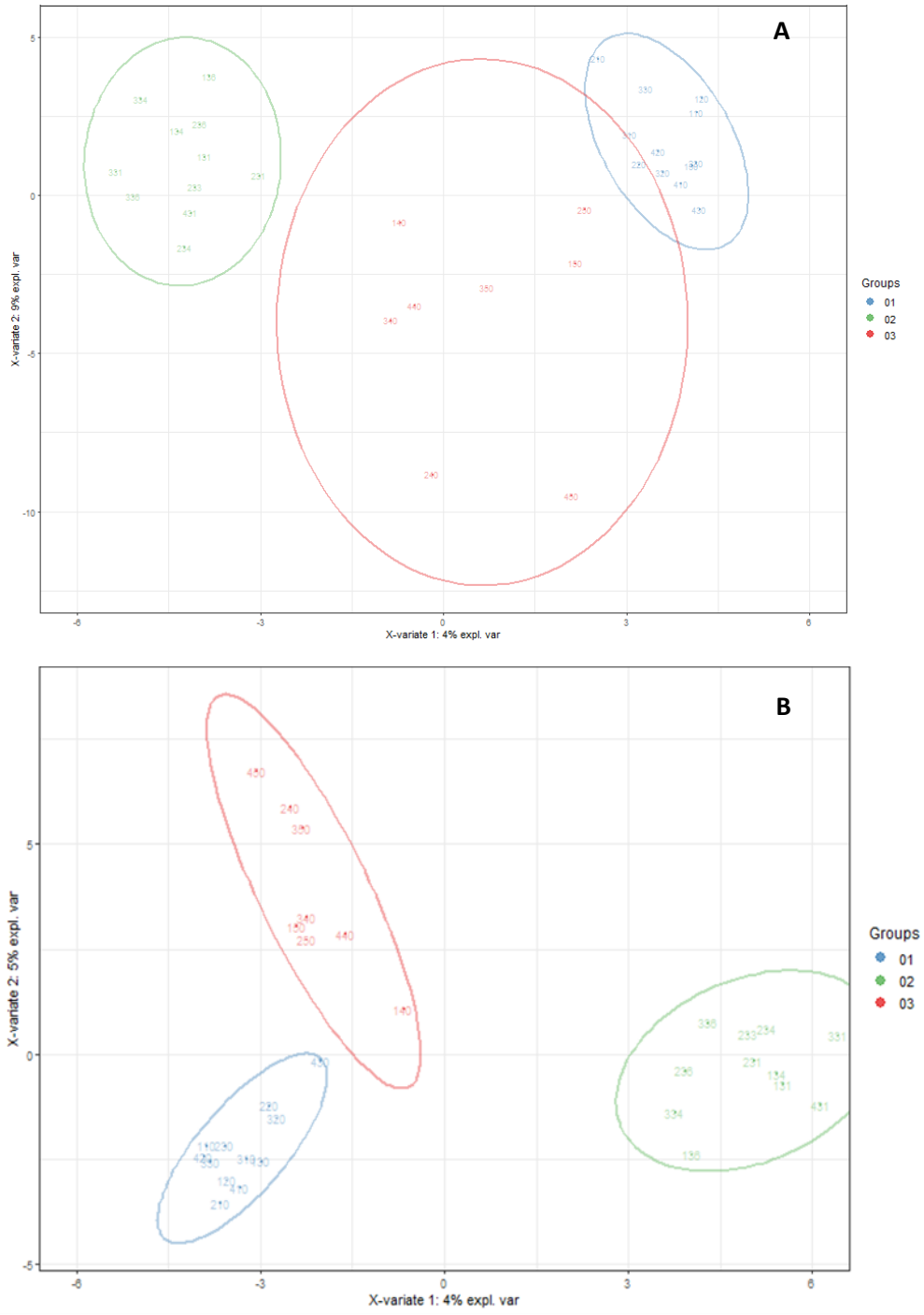

Figure S4. **Supervised Sparse Partial Least Squares Discriminant Analysis (sPLS-DA) plot of the chemical profiles of blood plasma of adult male (n=4, person 1 to 4) before and after administration of 1 g paracetamol.**
The samples were profiled in negative mode (A) and positive (B) modes by UHPLC-ESI-TOF-MS. Quality controls were removed from the sPLS-DA. **1:** *baseline group* = samples collected two days and just prior to intake of APAP (n=12), **2:** *1-6h group* = samples collected +1, +4, +6 hours after intake (n=11) and **3:** *+1-2 days group* = samples collected in the morning the subsequent two days (n=8).

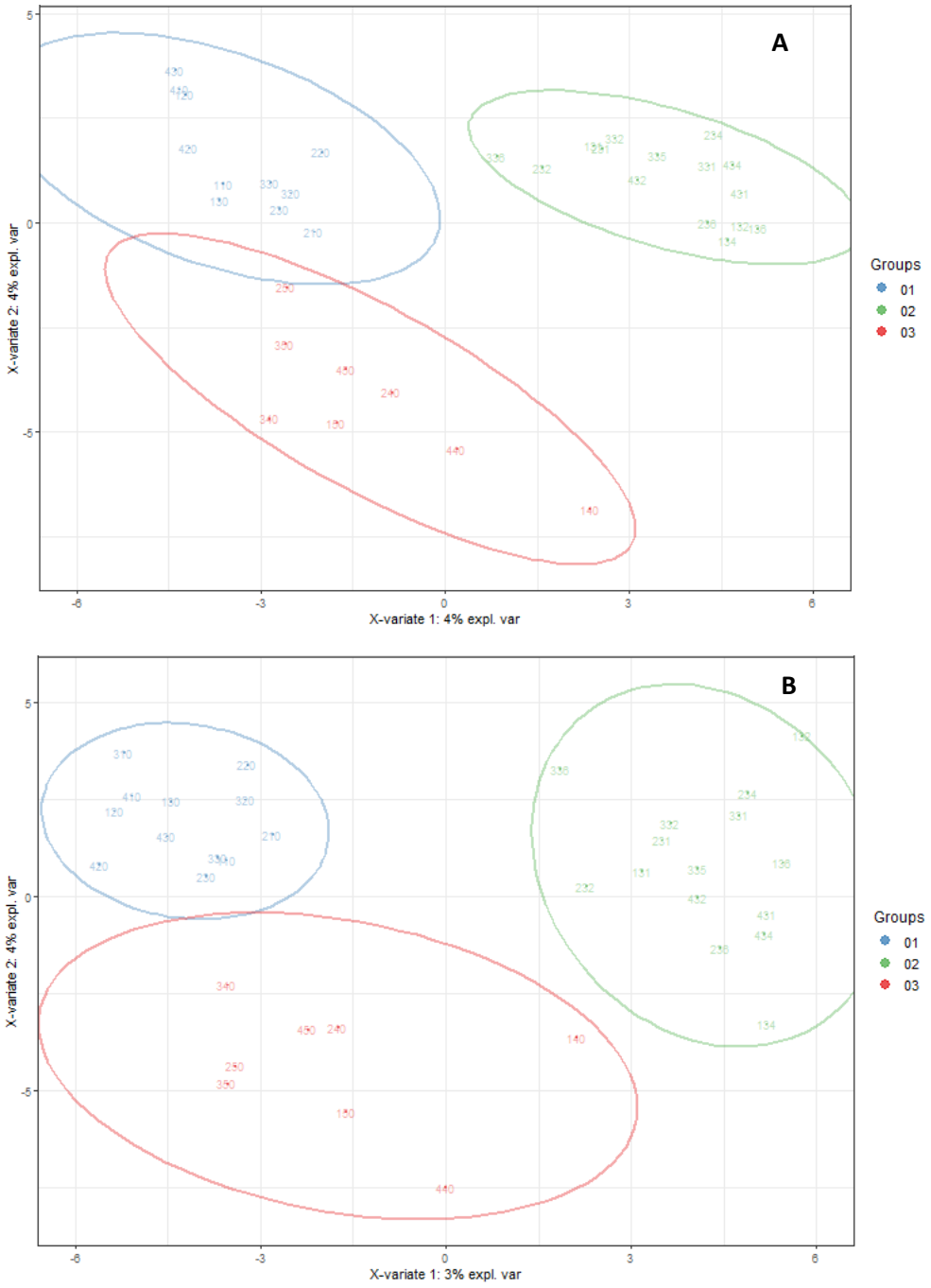

Figure S5. **Supervised Sparse Partial Least Squares Discriminant Analysis (sPLS-DA) plot of the chemical profiles of urine of adult male (n=4, person 1 to 4) before and after administration of 1 g paracetamol.** The samples were profiled in negative mode (A) and positive (B) modes by UHPLC-ESI-TOF-MS. Quality controls were removed from the sPLS-DA. **1:** *baseline group* = samples collected two days and just prior to intake of APAP (n=12), **2:** *1-6h group* = samples collected +1, +2, +4, +6 hours after intake (n=15) and **3:** *+1-2 days group* = samples collected in the morning the subsequent two days (n=8).

Supplementary Table 1: List of standards, internal standards and their suppliers used respectively for annotation and quality control

Compound	CAS no	Use	Supplier
Acetaminophen	103-90-2	Standard (annotation)	LGC-Dr Ehrenstorfer, Germany
Acetaminophen Dimer	98966-14-4	Standard (annotation)	LGC standards
Acetaminophen Mercapturate Disodium Salt	60603-13-6 free acid	Standard (annotation)	LGC standards
Acetaminophen-cysteine	64014-06-8	Standard (annotation)	LGC standards
4-Acetamidophenyl β-D-Glucuronide Sodium Salt	120595-80-4	Standard (annotation)	LGC standards
3-Hydroxyacetaminophen	37519-14-5	Standard (annotation)	LGC standards
3-Methoxy Acetaminophen	3251-55-6	Standard (annotation)	LGC standards
S-methyl-3-thioacetaminophen	37398-23-5	Standard (annotation)	LGC standards
Acetochlor-d11	34256-82-1	labelled standard	LGC, Germany
Azoxystrobin-d4	1346606-39-0	labelled standard	Cluzeau Info Labo, France
Carbamazepine-^{13}C6	N/A	labelled standard	Sigma-Aldrich, USA
Cotinine-d3	110952-70-0	labelled standard	LGC, Germany
Diclofenac-^{13}C6	1261393-71-8	labelled standard	Sigma-Aldrich, USA
Fluoxetine-d6	N/A	labelled standard	Sigma-Aldrich, USA
Cortisol-d4	73565-87-4	labelled standard	Sigma-Aldrich, USA
Ibuprofen-d3	121662-14-4	labelled standard	Sigma-Aldrich, USA
Imidacloprid-d4	1015855-75-0	labelled standard	LGC-Dr Ehrenstorfer, Germany
Ketoprofen-d3	159490-55-8	labelled standard	Sigma-Aldrich, USA
Paracetamol-d4	64315-36-2	labelled standard	LGC, Germany
Thiamethoxam-d4	1331642-98-8	labelled standard	LGC-Dr Ehrenstorfer, Germany
Tebuconazole-d6	N/A	labelled standard	LGC, Germany
Testosterone-d3	77546-39-5	labelled standard	Sigma-Aldrich, USA
Estrone-d4	53866-34-5	labelled standard	Trc, Canada

Supplementary Table 2: Parameters used for the pretreatment of mzml raw HRMS data using XCMS in an R environment.

Parameters	UHPLC-ESI-QTOF (X500R)
mzdiff	0.01
feature detection	centWave
prefilter intensity	10
bw	5
minfrac	0.5
Noise filter	0
mzwid	0.015
Parameters	UHPLC-ESI-QTOF (X500R)
feature detection	centWave
ppm	10
peakwidth(min,max)	(10,50)
snthresh	5
noise	10
prefilter	(3,100)
mzdiff	-0.001
fitgauss	FALSE
mzCenterFun	wMean
roiList	list()
integrate	1L
firstBaselineCheck	TRUE

Supplementary Table 3: Parameters used for the pretreatment of raw HRMS data using vendor software MarkerView.

Parameters	Value
Data to process	
Min Rt	1 min
Max Rt	55 min
Enhance peak finding	
Approximate LC peak width	20 s
Minimun intensity in peak counts	20
Perform bakcground substraction	yes
Chemical noise intensity multiplier	1.2
Alignment	
Retention time tolerance	1 min
Mass tolerance	10 ppm
Filtering	
Maximun number of peaks	10 000
Intensity threeshold	100
Remove peaks < 3 samples	NO
Isotope filtering	Remove isotops (keeping peaks with unkonw status)

Supplementary Table 4: Proportion of signals present in all quality controls (QCs) with coefficients of variation (CVs) for the absolute and normalized area (total signal) below 30% in plasma and urine according to the method of Want et al. (2010).

PLASMA (n=6, QCs)		
	NEGATIVE MODE	
	Absolute area	Normalised area
Number of signals present in all QCs	3727	3727
Proportion (%) compared to total number	99.9	99.9
Number of signals with a CV (area) <30%	3159	3151
Corresponding %	84.8	84.6
	POSITIVE MODE	
	Absolute area	Normalised area
Number of signals present in all QCs	2644	2644
Proportion (%) compared to total number	100.0	100.0
Number of signals with a CV (area) <30%	2269	2271
Corresponding %	85.9	85.9

URINE (n=9, QCs)		
	NEGATIVE MODE	
	Absolute area	Normalised area
Number of signals present in all QCs	7213	7214
Proportion (%) compared to total number	99.9	99.9
Number of signals with a CV (area) <30%	6141	6169
Corresponding %	85.1	85.4
	POSITIVE MODE	
	Absolute area	Normalised area
Number of signals present in all QCs	6403	6402
Proportion (%) compared to total number	100.0	99.9
Number of signals with a CV (area) <30%	5494	5520
Corresponding %	85.8	86.2

E. J. Want, I. D. Wilson, H. Gika, G. Theodoridis, R. S. Plumb, J. Shockcor, E. Holmes, J. K. Nicholson. Global metabolic profiling procedures for urine using UPLC MS. Nat. Protoc. 2010, 5, 1005

Supplementary Table 5: Coefficient of variation of of mean area of labelled internal standards in quality controls (QCs) in plasma (n=6 QCs) and urine (n=9 QCs) injected onto UHPLC-ESI-QTOF for the metabolomics analyses.

	Mean	Standard deviation	Coefficient of variation
Plasma*			
Cortisol d4	41661.7	2694.1	6.5
Imidacloprid d4	9269.7	720.6	7.8
Acetochlor d11	4824.8	337.7	7.0
Carbamazepine 6Ct	60861.7	2691.9	4.4
Azoxystrobin d4	159200.0	7744.7	4.9
Cotinine d3	3154.0	458.0	14.5
Estrone d4	30203.3	1374.1	4.5
Fluoxetine d6	18800.0	1196.4	6.4
Ketoprofen d3	23818.3	1110.8	4.7
Paracetamol d4	6298.0	1146.4	18.2
Tebuconazole d6	101368.3	3679.7	3.6
Thiamethoxam d4	8393.2	349.5	4.2
Diclofenac 6Ct	6727.7	215.7	3.2
Ibuprofen d3	N/A	N/A	N/A

	Mean	Standard deviation	Coefficient of variation
Urine			
Cortisol d4	827644.4	34659.3	4.2
Imidacloprid d4	185300.0	7592.3	4.1
Acetochlor d11	312755.6	7757.0	2.5
Carbamazepine 6Ct	1675888.9	47210.8	2.8
Azoxystrobin d4	6708111.1	70234.3	1.0
Cotinine d3	257611.1	20786.8	8.1
Estrone d4	790988.9	40977.9	5.2
Fluoxetine d6	2043888.9	82776.0	4.0
Ketoprofen d3	886455.6	38838.1	4.4
Paracetamol d4	111066.7	5762.8	5.2
Tebuconazole d6	4068666.7	137925.7	3.4
Testosterone d3	2357666.7	86333.7	3.7
Thiamethoxam d4	105417.8	7318.3	6.9
Diclofenac 6Ct	187485.7	5768.7	3.1
Ibuprofen d3	15082.9	235.9	1.6

* Testosterone d3 was not included in the internal standard solution in plasma

Supplementary Table 6: Annotation paramaters for APAP metabolites according to Schymanski et al. (2014).

					m/z						Rt	MS/MS profiles (SWATH)			
					Theoritical		Experimental		Δ ppm			Experimental		Standards/*In silico* models / literature	
												POS	NEG	POS	NEG
Name	Confid. Level [1]	InChI	CAS	Formula	M+H	M-H	M+H	M-H				MS/MS			
Parent and dimer															
acetaminophen (APAP)	**1**	InChI=1S/C8	103-90-2	C8H9NO2	152.0706	150.0561	152.0705	150.0557	-0.7	-2.3	5.0	65.0387, 80.0502, 93.0338, 110.0602	78.0349, 107.0376	65.0401, 80.0509, 93.0348, 110.0607	78.0350, 107.0372
Direct phase II reactions (Glu and S)															
Acetaminophen sulfate (APAP-S)	**2a**	InChI=1S/C8	10066-90-7	C8H9NO5S	232.0274	230.0129	232.0277	230.0127	1.3	-0.9	4.8		79.9570, 107.0370, 150.0559		79.9570, 107.0374, 150.0556
Acetaminophen glucuronide (APAP-Glu)	**1**	InChI=1S/C1	16110-10-4	C14H17NO8	328.1027	326.0881	328.1028	326.0880	0.3	-0.4	3.9	110.0602, 134.0605, 152.0702	107.0371, 113.0239, 150.056	110.0607, 134.0606, 152.0712	107.0374, 113.0242, 150.0557
Catechol pathway (phase I + II)															
3-hydroxyacetaminophen (3-OH-APAP)	**1**	InChI=1S/C8	37519-14-5	C8H9NO3	168.0655	166.0510	n.d.	166.0505	n.a.	-3.0	4.9		125.0243, 150.0556		125.0243, 150.0557
3-hydroxyacetaminophen sulfate (3-OH-APAP-S)	**2a**	InChI=1S/C8	53446-14-3	C8H9NO6S	248.0223	246.0078	248.0234	246.0079	4.4	0.4	4.6		79.9569, 122.0250, 148.405, 166.0508		79.9570, 122.0248, 148.404, 166.0510
3-methoxyacetaminophen glucuronide (3-OCH_3-APAP-Glu)	**2a**	InChI=1S/C1	52092-55-4	C15H19NO9	358.1132	356.0987	358.1131	356.0976	-0.3	-3.1	4.6	108.,0440, 140.0713, , 182.0807	85.0291, 113.0238, 180.0665	138.0550, 182.0812	85.0292, 113.0242, 180.0666
Mercapturate pathway (phase I + II)															
3-(Cystein-S-yl)acetaminophen (APAP-Cys)	**1**	InChI=1S/C1	53446-10-9	C11H14N2O4S	271.0747	269.0602	271.0742	269.0600	-1.8	-0.6	4.5	140.0169, 166.0314, 182.0869, 208.0427, 225.0697		140.0170, 166.0327, 182.0268, 208.0426, 225.0698	
Acetaminophen mercapturate (NAC-APAP)	**1**	InChI=1S/C1	52372-86-8	C13H16N2O5S	313.0853	311.0707	313.0847	311.0696	-1.9	-3.5	5.3	208.0421, 225.0691, 271.0742,	128.0356, 138.0011, 182.0273	208.0426, 225.0692, 253.0647,	128.0353, 138.0019, 182.0281
Acetaminophen mercapturate sulfoxide (NAC-O-APAP)	**2b**		n.a.	C13H16N2O6S	328.0729	327.0656	328.0737	327.0656	2.4	0.0	4.7		198.0227		198.023
Thiomethyl shunt pathway															
3-thioacetaminophen glucuronide (SH-APAP-Glu)	**2b**		n.a.	C14H17NO8S	360.0748	358.0602	360.0760	358.0595	3.3	-2.0	4.9		85.0293, 113.0240, 182.0280		85.0292, 113.0242, 182.0281
S-methyl-3-thioacetaminophen (S-CH_3-APAP)	**1**	InChI=1S/C9	37398-23-5	C9H11NO2S	198.0583	196.0438	n.d.	196.0438	n.a.	0.0	5.5		138.0020, 165.9965, 181.0202		138.0014, 165.9963, 181.0205
S-methyl-3-thioacetaminophen sulfate (S-CH_3-APAP-S)	**2b**	InChI=1S/C9	78194-51-1	C9H11NO5S2	278.0151	276.0006	n.d.	276.0004	n.a.	-0.7	5.2		79.9560, 138.0016, 165.9959, 181.0204, 196.0437		79.9570, 138.0017, 165.996, 181.0206, 196.0436
S-methyl-3-thioacetaminophen glucuronide (S-CH_3-APAP-Glu)	**2b**	InChI=1S/C1	78180-86-6	C15H19NO8S	374.0904	372.0759	374.0930	372.0753	7.0	-1.6	4.9		85.0291, 113.0242, 138.0019, 165.996, 181.0196, 196.0430		85.0292, 113.0242, 138.0017, 165.996, 181.0206, 196.0436
S-methyl-3-thioacetaminophen sulphoxide sulfate (SO-CH_3-APAP-S)	**2b**		n.a.	C9H11NO6S2	294.0101	291.9955	294.0131	291.9945	10.2	-3.4	4.8		79.9562, 122.0247, 155.0031, 180.0130, 212.0383		79.9570, 122.0247, 155.0031, 180.0130, 212.0387
S-methyl-3-thioacetaminophen sulphoxide glucuronide (SO-CH_3-APAP-Glu)	**2b**		n.a.	C15H19NO9S	390.0853	388.0708	390.0869	388.0707	4.1	-0.3	4.4		85.0293, 113.0240, 122.0249, 155.0028, 180.0121; 212.0382		85.0292, 113.0242, 122.0247, 155.0031,180.0130, 212.0387

[1] Confidence level according to Schymanski, E. L. et al.. Environ Sci Technol 48, 2097-2098, doi:10.1021/es5002105 (2014)

1 = confirmed structure: confirmation via appropriate measurement of a reference standard with MS, MS/MS and retention time matching.

2a = probable structure: matching literature or library spectrum data where the spectrum-structure match is unambiguous.

2b = diagnostic: no standard or literature information is available for confirmation. Evidence is diagnostic MS/MS fragments and/or ionization behavior, parent compound information and the experimental context (here APAP metabolites after exposure to parent compound).